Solar Energy 299 (2025) 113793

Contents lists available at ScienceDirect

Solar Energy

journal homepage: www.elsevier.com/locate/solener

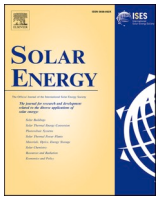

Evaluation of the environmental performance of an innovative solar thermal system applied to the industrial sector: a case study

Lisa Baindu Gobio-Thomas [a], Mohamed Darwish [b], Antonio Rovira [c], Ruben Abbas [d], Juan Pedro Solano [e], Jose Munoz Camara [e], Peter Kew [f], Krzysztof Naplocha [g], Valentina Stojceska [a,h,*]

[a] Brunel University London, College of Engineering Design and Physical Sciences, Department of Mechanical and Aerospace Engineering, Kingston Lane, Uxbridge UB8 3PH, United Kingdom
[b] Brunel University London, College of Engineering Design and Physical Sciences, Department of Electronic & Electrical Engineering, Kingston Lane, Uxbridge UB8 3PH, United Kingdom
[c] Universidad Nacional de Educación a Distancia (UNED), Juan del Rosal 12, Madrid 28040, Spain
[d] Universidad Politécnica de Madrid (UPM), José Gutiérrez Abascal 2, Madrid 28006, Spain
[e] Universidad Politécnica de Cartagena (UPCT), Edif. La Milagrosa, Cartagena CP30202, Spain
[f] Heriot Watt University, Edinburgh EH14 4AS Scotland, United Kingdom
[g] Wroclaw University of Science and Technology, Department of Lightweight Elements Engineering, Foundry and Automation, Wrocław 50-370, Poland
[h] Brunel University London, Institute of Energy Futures, Centre for Sustainable Energy Use in Food Chains, Uxbridge, Kingston Lane, Uxbridge UB8 3PH, United Kingdom

ARTICLE INFO

Keywords:
Environmental assessment
Solar thermal plants
Rotary fresnel solar collector

ABSTRACT

An environmental assessment of an innovative solar thermal technology called ASTEP has been performed. ASTEP consists of three main elements: a novel rotary Fresnel Sundial, thermal energy storage (TES) and the controls. It supplies solar thermal energy to industrial processes of maximum 400 °C. This energy source has been implemented to two end-users, Mandrekas and Arcelor Mittal, located in the regions with low and high latitudes. The results revealed that manufacturing of the ASTEP system had the most significant environmental impact, followed by the operation, transportation and waste disposal. Within the manufacturing phase, TES components had the highest environmental impact. This was primarily due to the greater quantity of materials and energy required for TES manufacturing compared to the other components. When applied to the end-users, ASTEP system demonstrated notable reduction of CO_2 emissions by 9.7 tonnes for MAND and 8.3 tonnes for AMTP. Furthermore, higher GHG emissions savings of 332 tonnes for MAND and 182 tonnes for AMTP could be achieved when the system's capacity is increased to 950 MWh/year and 609 MWh/year, respectively. The research demonstrated that the incorporation of the ASTEP system into industrial processes would result in a significant reduction of their environmental impact.

1. Introduction

The continued rise in world population, industrial activities and socio-economic development has resulted in significant increase in energy demand and consumption, a trend that is likely to continue in future years [1]. Oil, coal and gas are still the dominant fuels used to provide energy in different sectors across the world. However, fossil fuels are non-renewable and release significant greenhouse gas emissions into the atmosphere resulting in global warming, air pollution and negative human health impacts. Therefore, it is essential that alternative energy sources like renewable energy are used. Governments worldwide are under increasing pressure to reduce GHG emissions and limit global warming to about 1.5 °C as stated in the United Nations Framework Convention on Climate Change (UNFCCC) and 2015 Paris Agreement [2]. As a result, the EU Parliament and its member states have agreed to reduce carbon emissions by at least 55 % by 2030, compared to 1990 levels, to achieve climate neutrality by 2050 [3]. The EU's 2030 climate and energy framework target includes increasing the share of renewable energy to 32 % [4]. Consequently, a number of incentives such as the "Just Transition Mechanism", "Innovation Fund" and "Horizon Europe" have been provided to EU member states to encourage the adoption of renewable energy technologies, which in turn will reduce GHG

* Corresponding author.
E-mail address: Valentina.Stojceska@brunel.ac.uk (V. Stojceska).

https://doi.org/10.1016/j.solener.2025.113793
Received 29 November 2024; Received in revised form 6 July 2025; Accepted 12 July 2025
Available online 26 July 2025

emissions in industries and other sectors.

The industrial sector accounts for the third largest share of energy consumption in the EU [5]. Natural gas, oil and electricity are predominantly main energy sources used in the EU industrial sector [6]. Renewable energy currently contributes about 22 % of the total EU energy demand that is mainly used for heating and cooling processes, while the rest is provided by fossil fuels, particularly for industrial processes that require temperatures above 400 °C [7]. Chemicals and petrochemical industry are the most energy-consuming industrial sectors, followed by paper, non-metallic minerals, iron/steel, food and tobacco sectors [8]. Non-metallic minerals, iron/steel, chemicals & petrochemicals produce the largest amount of carbon emissions, representing around 20 % of total industry emissions each. Half of all the emissions in these energy-intensive industries sector in the EU are being caused by the heating of fossil fuels in furnaces for high-temperature processes [9,10]. The use of thermal energy in the industrial sector increased by 24 % from 1995 to 2019 [6]. This increased demand for heat in the industrial sector can be met by solar thermal technologies which are promising alternatives to fossil fuels for the provision of heating and cooling for industrial processes, thereby reducing their GHG emissions and contributing to the decarbonisation of EU industries.

The environmental performance is a critical step in quantifying the environmental impact of renewable energy technologies which is usually achieved through life cycle assessment (LCA). Several studies have conducted environmental LCA of concentrated solar thermal plants that provide thermal energy at high temperatures up to 400 °C and above. However, most of these studies have focused on the LCA of concentrated solar thermal plants mainly used for electricity production [11–15]. There were only a few studies found in the reviewed literature that conducted environmental LCA of solar thermal technologies providing thermal energy of 150°C and above, for industrial processes and not only for electricity generation [16–19]. Furthermore, there were limited studies on the environmental LCA of linear Fresnel solar thermal technologies compared to parabolic trough and solar tower systems with only a few studies from the reviewed literature assessed the environmental performance of linear Fresnel solar thermal plants [18,20–23]. From these studies, only three studies specifically performed environmental life cycle assessment of linear Fresnel solar thermal technologies [18,20,24]. Two of these were published ten years ago, while only one study was published recently. Therefore, there's a need for more recent studies on the environmental LCA of Fresnel solar thermal techonolgies. Hang et al. [18] evaluated the energy consumption and GHG emissions of a 125 MW linear Fresnel plant. Cumulative energy demand (CED) and IPCC GWP (100a) were used to assess the environmental impact of the plant, resulting in 160,278 GJ for the energy consumption and 31 g CO_2eq/kwh for its GHG emissions. Kuenlin et al. [20] used Impact 2002 + to compare the environmental impact of a linear Fresnel, parabolic-trough, solar tower and solar dish plants. The results showed that the environmental impact of the linear Fresnel plant was mainly due to the manufacturing of its solar field and had the highest impact on human health, followed by resources, climate change and then on ecosystem quality. Batuecas et al. [24] used the International Reference Life Cycle data (ILCD) impact assessment to assess the environmental impact of the construction and operation phase of a linear Fresnel solar field which consists of primary and secondary solar reflectors. The results showed that at optimal configurations of the LFR solar field, the climate change impact was 0.18kgCO_2 eq/kwh, ozone depletion was 1.3x 10^{-8} kg CFC-11 eq/kwh and particulate matter was 1.8 × 10^{-4} kg $PM_{2.5}$ eq/kwh. Hang et al. [18] used CED to assess the energy demand of the LFR plant because this impact assessment method is usually used to evaluate the energy consumption of a system or product. IPCC GWP (100a) was also used to compute the GHG emissions of the LFR plant. Kuenlin et al. [20] used Impact 2002 + to assess the human health, ecosystem quality, climate change and resources of the different solar thermal technologies, including LFR. Batuecas et al. [24] used the International Reference Life Cycle data (ILCD) impact assessment in their study and stated that this method was recommended by the European Commission Joint Research Centre for life cycle impact assessment (LCIA). The lack of published studies on environmental LCA of Fresnel solar thermal technologies used for thermal energy production has been observed in studies by Batuecas et al. [24] and Gobio-Thomas et al. [25].

Therefore, this study extends to the exisitng but limited body of literature concerning the environmental LCA of Fresnel solar thermal systems, providing thermal energy up to 400°C for industrial processes. A key novelty of the solar thermal technology assessed in this study is that it is a rotary Fresnel solar collector where both the Fresnel solar collectors and platform can rotate simultaneously capturing more of the solar irradiance, which is important for locations at high latitude but with low solar irradiance. Consequently, this novel rotary Fresnel solar thermal system can be used at both high and low latitude locations to provide thermal energy for industrial processes requiring temperatures up to 400 °C [26]. This study also makes projections about the potential GHG emissions reduction savings that can be achieved when this novel solar thermal system is used to provide thermal energy in large capacities to industrial processes. To the best of the authors' knowledge, there is no existing literature or published research paper that explores the environmental impact of a rotary Fresnel solar thermal system. Therefore, this study provides a key contribution to the limited body of literature available on the environmental performance of Fresnel solar thermal technologies, with a specific focus on rotary Fresnel solar thermal systems.

2. Description of ASTEP system

The ASTEP system is an innovative solar thermal technology consisting of three main subsystems; the novel rotary Fresnel Sundial solar collector, the thermal energy storage and the control system. The ASTEP system has a great potential to reduce GHG emissions in various industries by suppling green energy for high- temperature processes to 400 °C to companies located at both low and high latitudes. This study will consider its application to two end users; Mandrekas (MAND) and ArcelorMittal (AMTP) [27]. Mandrekas is a family owned dairy company located in Corinth, Greece and is located in a region at a low latitude of 37.93 N. The company produces different types of yogurt, yogurt-based dressings and milk desserts. Their production process requires different temperatures of up to 175 °C for milk pasteurization and 5 °C for the refrigeration of the dairy products. The ASTEP system will be used to provide thermal energy for the pasteurization and cooling processes using an absorption chiller [26]. Fig. 1 shows the schematic diagram of the ASTEP solar thermal system for Mandrekas (MAND). The SunDial's collector mirrors reflect the solar energy to an elevated receiver system and heats up the thermal oil in its receiver tubes. The heated thermal oil flows to the thermal energy storage tank where the thermal energy is stored and released when needed. When it is released, the hot thermal oil flows to the solar assisted cooling unit (absorption chiller) and the solar assisted heating (steam drum & heat exchanger). The heated thermal oil provides the absorption chiller in the solar assisted cooling unit with thermal energy which is used to chill the coolant (water and glycol). This enables the absorption chiller to provide the cooling demand of 5 °C for the refrigeration of the dairy products. The hot thermal oil also flows into the solar assisted heating unit (steam drum & heat exchangers) and provides thermal energy to the steam drum to produce steam for the pasteurisation of the milk and other processes in the dairy factory. The temperature of the thermal oil in the pipes drops and flows back to the SunDial unit.

ArcelorMittal is the world's leading steel company and its metal processing plant is located in Iasi, Romania, at a high latitude of 47.1 N. The company manufactures welded steel tubes for many diverse applications. The steel tubes are colour coated using a thin layer of coloured protective and decorative material covering the whole tube's external surface. In order to apply this coating on the tubes, the steel tubes need to be pre-heated to a temperature of 230 °C. Therefore, the ASTEP

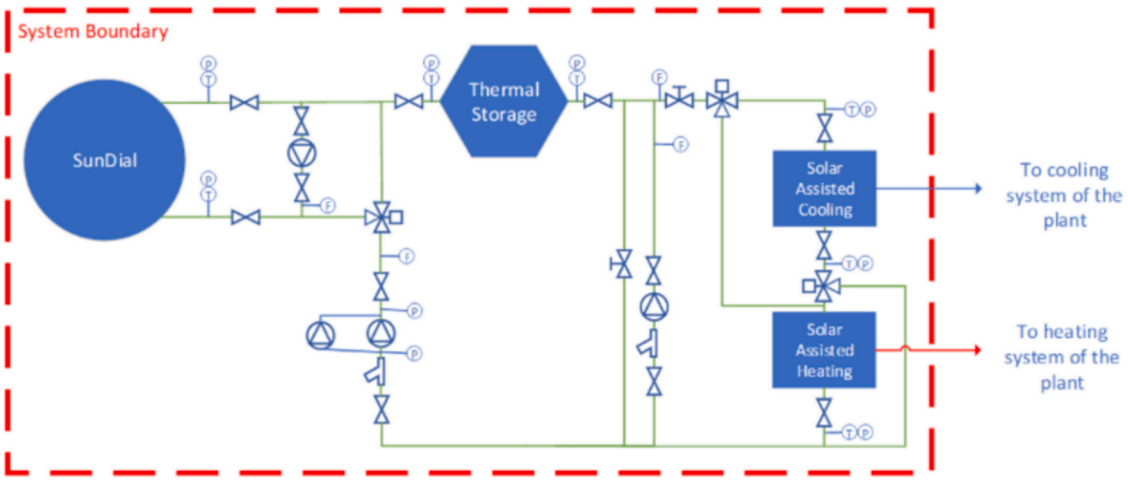

Fig. 1. Integration of ASTEP solar thermal system with MAND's processes.

system will be used at AMTP to provide thermal energy to preheat the manufactured tubes before their colour coating process [28]. Fig. 2 presents the schematic diagram of the ASTEP system integrated with AMTP's processes. The SunDial's collector mirrors reflect the solar energy to an elevated receiver system and heats up the thermal oil in its receiver tubes. The heated thermal oil flows to the thermal energy storage tank where the thermal energy is stored and released when needed. When it is released, the hot thermal oil flows to the solar assisted heating unit (heat exchangers). The heat exchangers heat up the air and the hot air goes into the oven which heats up the metal pipes that the factory is producing. The temperature of the thermal oil drops and flows back to the SunDial unit.

2.1. Rotary fresnel sundial solar collector

The Sundial solar collector is a Rotary Fresnel Collector (RFC), consisting of short, parallel Fresnel collectors installed on top of a rotary platform which tracks the sun. The Sundial is compact and fast to manufacture and install, thereby reducing its installation, maintenance and operation requirements [26]. Two different designs of the Sundial have been developed to operate at low latitude and high latitude locations (Fig. 3):

- Low-Latitude Sundial Design: This is presented in Fig. 3a and will be installed at MAND. It consists of a single-axis tracking system where only the platform rotates to capture the solar irradiance whilst the mirrors are stationary on the platform. The platform is a square, measuring 8.6 m by 8.6 m and the receivers are 8 m long as shown in Fig. 3a. The mirrors field is tilted longitudinally and the mirrors are shorter than the receivers. The lateral mirrors which are 4 m long, are shorter than the central mirrors which are 6 m long, to reduce end losses and increase the Sundial's efficiency [26].
- High-Latitude Sundial Design: This is presented in Fig. 3b and will be installed at AMTP. It consists of a double-axis tracking system, where the platform rotates to maintain the sun within the field cross section resulting in a significant reduction of the cosine losses. The platform is a square, measuring 8.1 m by 8.1 m and the receivers are 8 m long as shown in Fig. 3b. The mirrors which are 8 m long also rotate to track the sun's varying elevation and the mirror's axes and receivers are located in two tilted to minimise shading losses [26]. In the high latitude SunDial design, the platform rotates to keep the sun in the field's cross section, and each individual mirror also tracks the sun's elevation. This design enables the SunDial to achieve the same energy production of 27.8 MW h at a high latitude of 47.1 ∘N as it does at low latitude of 37.9 ∘N [26].

2.2. Thermal energy storage (TES)

The thermal energy storage (TES) that is the second part of the ASTEP system, is based on phase change materials (PCM) with a mixture of sodium and potassium nitrate salts ($NaNO_3$-KNO_3) as the PCM materials. The TES stores the excess solar thermal energy produced by the

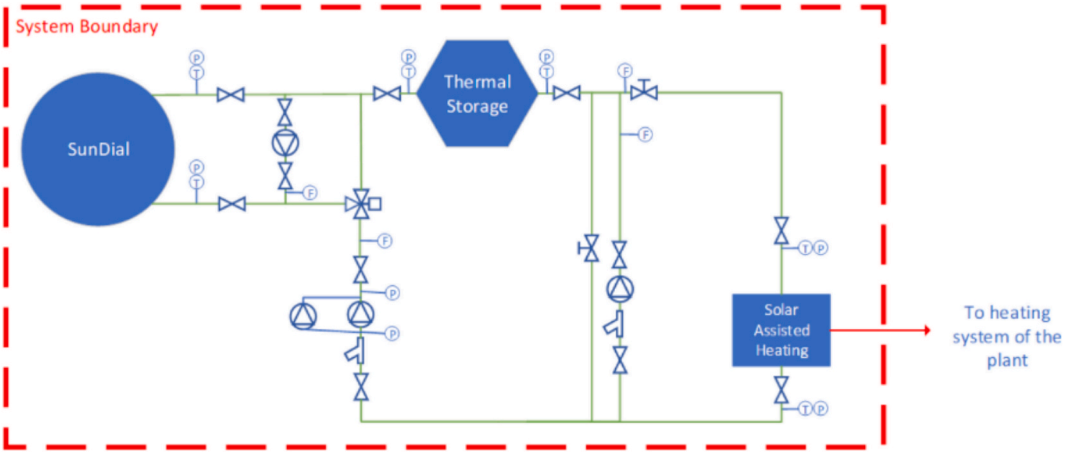

Fig. 2. ASTEP solar thermal system integrated with AMTP's processes.

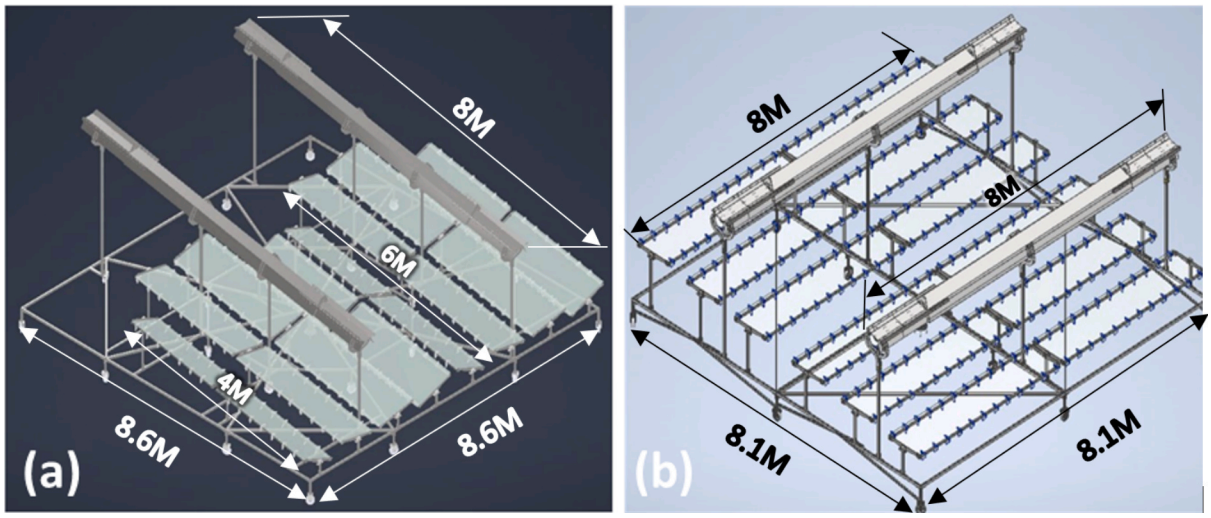

Fig. 3. Design of Sundial Concentratiors for (a) Mandrekas – 37.93 N & (b)ArcelorMittal – 47.1 N [26].

Sundial during peak production hours, and deliver it to the end user when it is required. The passive design of the TES consists of honeycomb structures which are in a shell enclosure (Fig. 4a) and have the form of multi tubes (Fig. 4b) with integrated elements enhancing the heat transfer. The heat transfer fluid (HTF) flows through the inside tubes, and the PCM is stored at the shell side, filling the structure created by the honeycomb. This active design makes it possible to control the stored thermal energy during charging and to release it during discharging [27].

2.3. Control system

The control system is based on a programmable logic control (PLC) unit (Fig. 5) and will ensure that the heat supply remains within the process specifications (temperature, pressure, flow rates). This will be achieved through centralised control and flexible operation of the system [27]. The system will also have a user control interface where the operator will be able to check in real time the condition of the system. The PLC unit will transmit data throughout the system and the sensors and actuators will send and receive signals from the PLC to ensure the smooth operation of the ASTEP system [30].

3. Methodology

The environmental impact of the novel ASTEP technology was conducted through life cycle assessment (LCA) using SimaPro 9.2 software (Pre-Sustainability, Netherlands) and Eco-invent 3.6 database.

3.1. Life cycle assessment of ASTEP system

Life Cycle Assessment was used to quantify and evaluate the life cycle of the ASTEP system including raw materials extraction, transportation of materials & components, manufacturing of the components and disposal of the components at their end of life stage. Eco-Indicator 99, IPCC Global Warming Potential (GWP) 2021 and Cumulative Energy Demand were the life cycle impact assessment methods used in this study.

The LCA study consists of the four iterative phases [31]:

(i) Goal & Scope of study.
(ii) Life Cycle Inventory (LCI) Analysis.
(iii) Life Cycle Impact assessment (LCIA).
(v) Interpretation of Results.

3.1.1. Goal & Scope of study

The aim of the study is to conduct an environmental life cycle assessment of the ASTEP system which provides thermal energy to the industrial processes of MAND and AMTP. The ASTEP system provides up to 135 kWh per day and 27.8 MWh of annual thermal energy for each end user, MAND & AMTP [26,32]. The functional unit of the ASTEP system is 1 kWh of thermal energy. The estimated lifetime of a linear

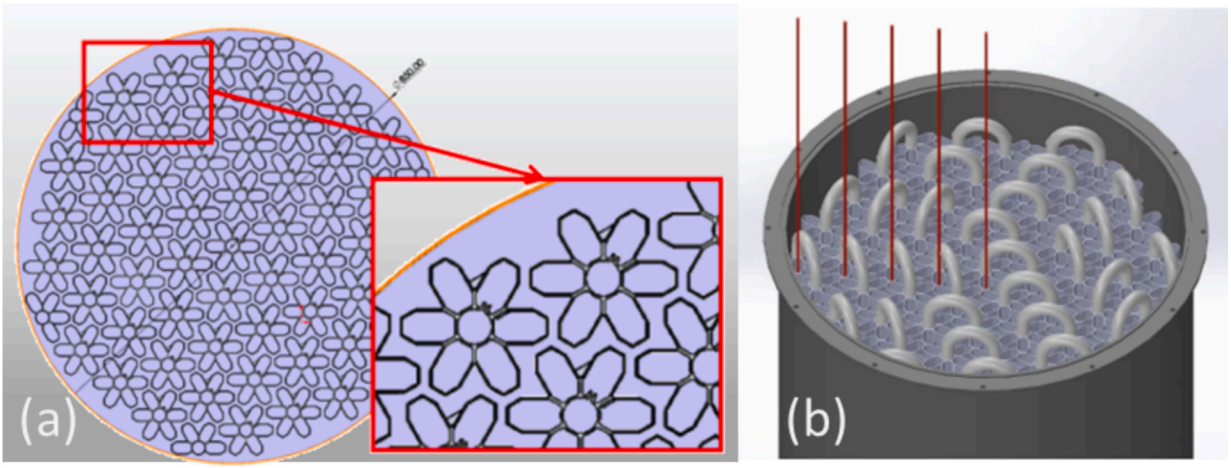

Fig. 4. Thermal Energy Storage (a) honeycomb design shell-side inserts & (b) multi-tubes & shell-side inserts inside TES tank [29].

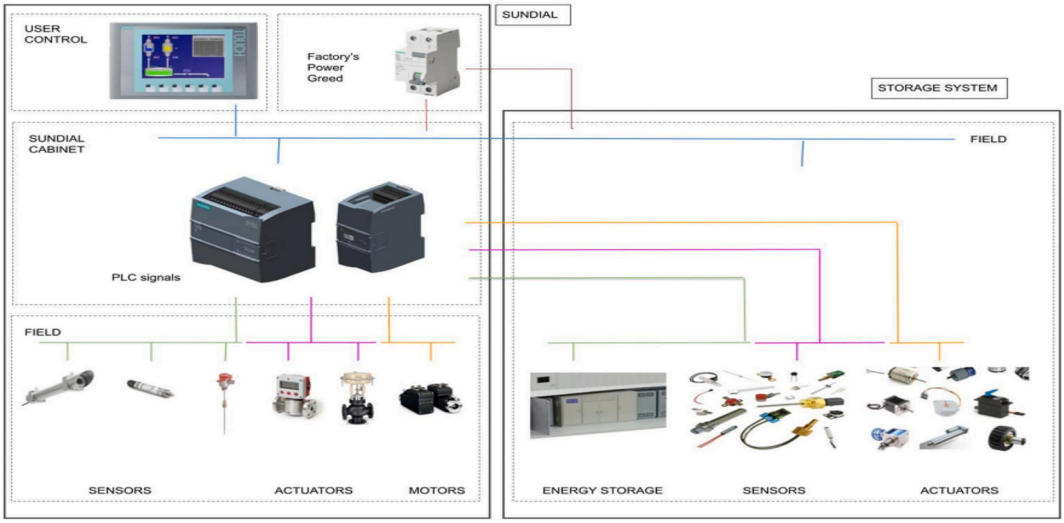

Fig. 5. Control system Architecture [30].

Fresnel plant is 30 years [33]. The lifetime of 30 years for the linear Fresnel plant was selected as this is the number of years typically used for the lifetime of solar thermal plants including linear Fresnel plants in the literature [18,33,34]. The system boundaries of the ASTEP system are shown in Fig. 6 and include the extraction of the raw materials, transportation of materials & components, manufacturing of the system components, operation and disposal of the components. The inputs are the energy consumed throughout the life cycle of the ASTEP system. The outputs are the thermal energy generated and air emissions produced throughout the life cycle of the system.

3.1.2. *Life cycle Inventory data of ASTEP system (MAND & AMTP)*

The life cycle inventory data for each part of the ASTEP system is presented in Table 1 which includes the type of components, materials and weight of the materials for the Sundial, TES, Controls and the platform structures. The designs of the Sundial units for MAND and AMTP are different due to their varying latitudes as shown in Fig. 3a and 3b. The TES design is the same for both MAND and AMTP, however, MAND's ASTEP system uses one TES tank compared to two TES tanks for AMTP. The initial design for the ASTEP system consisted of a total of 4 TES tanks; 2 TES tanks each for MAND and AMTP. AMTP used 2 TES tanks because achieving a high temperature at a location of high latitude

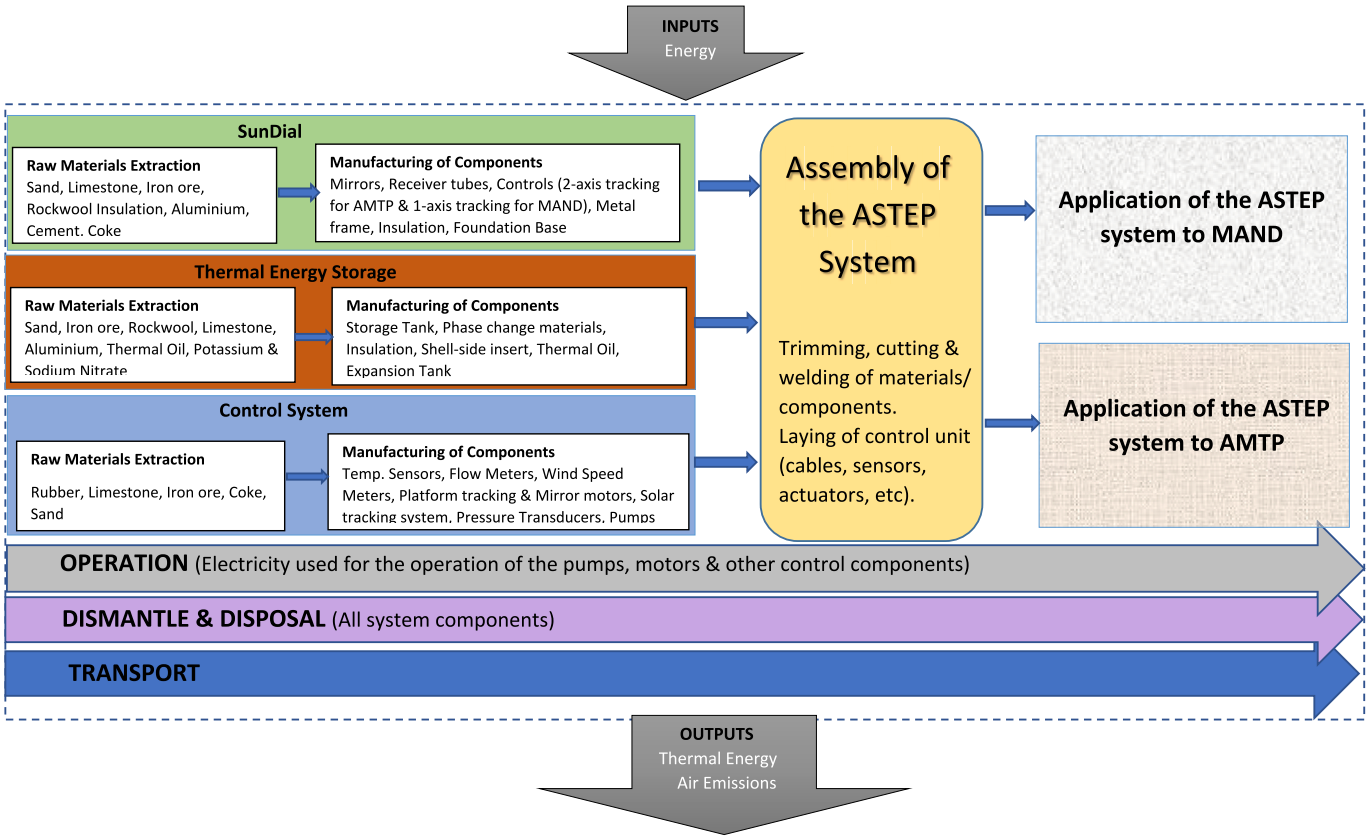

Fig. 6. System Boundaries of ASTEP system.

Table 1
Life Cycle Materials Inventory of ASTEP system (MAND & AMTP).

Components	Materials	Weight of materials (kg/litres)	
		MAND	AMTP
Sundial Components			
Mirrors (Standard)	Glass	356.25 kg	330 kg
Receiver Tubes	Steel	152.4 kg	152.4 kg
	Borosilicate glass jacket	70 kg	70 kg
Insulation of Pipes	Rockwool	27.4 kg	24.2 kg
Pipes	Steel	118 kg	107 kg
Support Structure	Aluminium	324 kg	322.8 kg
	Steel	1495.5 kg	1201 kg
Rotating Platform & Lateral Supports	Steel	3369.3 kg	2997.3 kg
Platform Structure	Concrete	2800 kg	2400 kg
	Steel	4300 kg	n/a
TES Components			
Storage Tanks	Steel	1000 kg	2000 kg
	Graphite	0.01 kg	0.02 kg
Phase Change Materials	Sodium Nitrate ($NaNO_3$)	505 kg	1,010 kg
	Potassium Nitrate (KNO_3)	600 kg	1,200 kg
Tubes	Steel	91.5 kg	183 kg
Shell-side Inserts	Aluminium	1,464 kg	2,928 kg
Insulation of Tank Walls	Rockwool	310 kg	620 kg
Expansion tank	Steel	74.5 kg	74.5 kg
Thermal oil	Therminol 59	218 L	250 L
Control Components			
Temperature Sensors	Steel	2.16 kg	2.43 kg
	Polyurethane (plastic)	0.24 kg	0.27 kg
Flow Meter	Steel	1.68 kg	5.04 kg
	Polyurethane (plastic)	0.48 kg	1.440 kg
	Copper	0.12 kg	0.36 kg
Pressure Transducers	Iron	0.182 kg	0.061 kg
	Chromium	0.051 kg	0.017 kg
	Nickel	0.036 kg	0.012 kg
	Manganese	0.008 kg	0.0025 g
	Copper	0.003 kg	0.001 kg
	Aluminium	0.003 kg	0.001 kg
Electrical Cabinets	Steel	300 kg	300 k g
	Polyvinyl chloride (PVC)	30 kg	30 kg
Speed pumps	Steel	0.03 kg	36 kg
	Iron	13.5 kg	18 kg
	Bronze	2.7 kg	3.6 kg
	Polyurethane (plastic)	5.4 kg	7.2 kg
Solar Tracking system	Steel	54 kg	54 kg
	Polyurethane (plastic)	9 kg	9 kg
	Copper	9 kg	9 kg
	Zinc	18 kg	18 kg
Mirror Tracking Motors	Steel	n/a	71.4 kg
	Copper	n/a	7.65 kg
	Polyurethane (plastic)	n/a	7.65 kg
Platform Tracking Motors	Steel	4.2 kg	4.2 kg
	Copper	0.9 kg	0.9 kg
	Polyurethane (plastic)	0.9 kg	0.9 kg
Windspeed meter	Steel	0.5 kg	0.5 kg
	Polyurethane (plastic)	3 kg	3 kg
Platform Structures			
Foundation	Concrete	2800 kg	2400 kg
	Steel	4300 kg	n/a

is more challenging. Therefore, using two TES tanks enables AMTP's ASTEP system to provide temperatures up to 230 °C during days of high solar irradiation but achieve more constant temperatures on regular days. The TES provides 5.8 h of thermal energy for each end-user, MAND and AMTP. The environmental impact of the platform structures designed for each of the end users, MAND and AMTP was also considered. The difference between these platform structures is that MAND's platform is higher at roof level with a large amount of steel and concrete used in its construction. In contrast, AMTP's platform is at ground level with a smaller amount of concrete used to construct it.

The Sundial components were transported from the suppliers and assembled in in Getafe, Spain, while the TES components were assembled in Cartegena, Spain. The components of the controls system were assembled in Madrid, Spain. The weight of the Sundial, TES and Controls components was multiplied by the distance from the various suppliers to their assembly locations and then to the end users, MAND in Greece and AMTP in Romania. The waste disposal method selected in SimaPro software (Pre-Sustainability) was the treatment of municipal solid waste (EU 27) which includes recycling of the materials at their end of life stage. The manufacturing data for the Sundial, TES, Controls components and the platform structures, the total transportation distance of the components from suppliers to each end-user and the waste disposal method were placed in SimaPro software to calculate the environmental life cycle impact of the ASTEP system. Data presented in Table 1 were placed in SimaPro software to calculate their environmental impact. Two different simulations were performed for the two end- users, MAND & AMTP. The LCA results were then exported to excel and the environmental performance of the ASTEP system for MAND and AMTP were analysed.

3.2. Calculation of current & future GHG emissions reduction of ASTEP

The annual current capacity of the ASTEP system for both MAND and AMTP is 27.8 MWh [26]. MAND's production process requires heat for pasteurization and cooling for the refrigeration of its products. It is estimated that half of the energy of the ASTEP system is used to provide heating and the other half is used to provide cooling for MAND's processes. The carbon intensity for LPG is 0.22 kg CO_2 per kWh [35] and the carbon intensity for electricity in Greece is 0.479 kg CO_2 per kWh [32]. AMTP only uses electricity for its processes, therefore, the AMTP's ASTEP system's annual capacity of 27.8 MWh was multiplied with the carbon intensity of 0.299 kg CO_2 per kWh for electricity in Romania [32] to obtain its current GHG emissions reduction when ASTEP system is used to provide thermal energy for AMTP's processes. This section presents the current and future GHG emissions of ASTEP system when applied to MAND and AMTP's processes.

3.2.1. Calculation of current GHG emissions reduction (ASTEP system)

This section presents the calculation of the current GHG emission reduction of MAND and AMTP's ASTEP system.

$$GHGemissionsreduction(MAND) = (CarbonintensityofLPG\&electricity) \times \frac{1}{2} annualcapacityofASTEPsystem \quad (1)$$

$$GHGemissionsreduction(AMTP) = Carbonintensityofelectricity \times annualcapacityofASTEPsystem \quad (2)$$

Eq. (1) was used to calculate the current GHG emissions reduction of the ASTEP system when applied to MAND's processes. Eq. (2) was used to calculate the current GHG emissions reduction of the ASTEP system

Table 2
Current GHG emissions reduction of ASTEP (MAND).

Total Carbon Intensity of LPG & Electricity (kgCO_2/kwh)	Half Annual Capacity of ASTEP system (MWh)	GHG emissions reduction (tonnes of CO_2 equivalent)
0.699	13.9	9.7

when applied to AMTP's processes.

Table 2 presents MAND's total carbon intensity, half annual capacity of ASTEP system and the current GHG emissions reduction of ASTEP system when applied to MAND's processes.

Table 3 presents AMTP's total carbon intensity, annual capacity of ASTEP system and the current GHG emissions reduction of ASTEP system when applied to AMTP's processes.

3.2.2. Calculation of energy demand (MAND)

This section presents the calculation of the energy demand of MAND processes. It also includes the conversion of MAND's LPG consumption (m^3) to MWh.

$$LPG(MWh) = (LPG(m3) \times calorificvalue \times correctionfactor)\tilde{A}\cdot conversionfactor \quad (3)$$

$$MAND'sTotalEnergyDemand(MWh) = LPG(MWh) + Electricity(MWh) \quad (4)$$

MAND and AMTP' annual energy demand was calculated from their annual LPG and electricity consumption provided by the project partners. Eq. (3) was used to convert the annual LPG consumption of MAND's processes from m^3 to MWh. Eq. (4) was used to calculate MAND's total energy demand. The LPG consumption of MAND's processes is 118,601 m^3 [36]. The calorific value of LPG is 94 MJ/m^3 [37]. The correction factor is 1.02264 and the conversion factor is 3.6 [38]. MAND's electricity consumption is 1,582.6 MWh [36].

Table 4 shows MAND's LPG consumption in m^3, the calorific value, correction factor, conversion factor and the annual LPG consumption in MWh.

Table 5 shows MAND's annual LPG consumption, electricity consumption and total energy demand.

3.2.3. Calculation of energy demand (AMTP)

This section presents the calculation of the energy demand of AMTP's processes. It also includes the conversion of AMTP's total energy demand from MJ/year to MWh.

$$TotalEnergyDemand(MWh) = TotalEnergyDemand(MJ/yr)\tilde{A}\cdot Conversionfactor \quad (5)$$

Eq. (5) was used to convert AMTP's total energy demand from MJ/yr to MWh. AMTP's total energy demand for heating the metal pipes is 846,000 MJ/year [36]. The conversion factor is 0.2778 [39].

Table 6 shows AMTP's total energy demand in MJ/yr, the conversion factor and the total energy demand in MWh.

3.2.4. Future prospective GHG emissions reduction

This section presents the calculation of the future prospective GHG emissions reduction when the ASTEP system is used to supply 20 % of the energy demand of MAND and AMTP's processes.

$$FutureGHGemissionsreduction(MAND) = 20\% \times MAND'senergydemand \times carbonintensityofLPG\&electricity \quad (6)$$

$$FutureGHGemissionsreduction(AMTP) = 20\% \times AMTP'senergydemand \times carbonintensityofelectricity \quad (7)$$

Table 3
Current GHG emissions reduction of ASTEP (AMTP).

Carbon Intensity of Electricity ($kgCO_2$/kwh)	Annual Capacity (MWh)	GHG emission reduction (tonnes of CO_2 equivalent)
0.299	27.8	8.3

Table 4
Conversion of LPG consumption from m3 to MWh (MAND).

LPG Consumption (m^3)	Calorific Value (MJ/m^3)	Correction factor	Conversion factor	LPG Consumption (MWh)
118,601	94	1.02264	3.6	3,166.9

Table 5
Total energy demand (MAND).

LPG (MWh)	Electricity (MWh)	Total Energy Demand (MWh)
3,166.9	1,582.6	4,748.9

Table 6
Conversion of total energy demand from MJ/yr to MWh.

Total Energy Demand (MJ/yr)	Conversion factor	Total Energy Demand (MWh)
846,000	0.2778	3,046.4

Eq. (6) was used to calculate the future GHG emissions of ASTEP system when used to supply 20 % of the energy demand of MAND's processes. Eq. (7) was used to calculate the future GHG emissions of ASTEP system when used to supply 20 % of the energy demand of AMTP's processes.

Table 7 presents the future prospective GHG emissions reduction of ASTEP system when used to provide 20 % of MAND's current energy demand.

Table 8 presents the future prospective GHG emissions reduction of ASTEP system when used to provide 20 % of AMTP's current energy demand. The future prospective GHG emissions reduction of the Sundials were calculated based on the Sundials providing 20 % of MAND and AMTP's current energy demand of 4,748.9 MWh and 3,046.4, respectively. This results in future prospective capacity of 950 MWh for MAND's ASTEP system and 609 MWh for AMTP's ASTEP system. It's estimated that half of the energy of the ASTEP system is used to provide heating and the other half is used to provide cooling for MAND's processes. The total carbon intensity of LPG and electricity (0.699 kg CO2 per kWh) in Greece was multiplied by 475 MWh (half of the prospective increased capacity of 950 MWh) to obtain the future GHG emissions reduction of 332 tonnes of CO_2/kwh when the ASTEP system is applied to MAND's processes. AMTP only uses electricity for its processes, therefore, the carbon intensity of electricity which is 0.299 kg CO_2 equivalent in Romania was multiplied by its prospective increased capacity of 609 MWh to obtain the future GHG emissions reduction of 182 tonnes CO_2 equivalent when the ASTEP system is applied to AMTP's industrial processes in larger capacity.

4. Results & discussion

This section presents the environmental impact results of the ASTEP system for MAND and AMTP and discusses the findings.

4.1. Human Health, ecosystem quality & resources impact of the components of ASTEP system

Fig. 7 illustrates the human health, ecosystem quality & resources impact of the components of MAND's ASTEP system. It can be seen that

Table 7
Future Prospective GHG emissions reduction (MAND).

20 % of MAND's energy demand (MWh)	Carbon intensity of LPG & electricity ($kgCO_2$/kwh)	Future Prospective GHG emissions reduction (tonnes CO_2 equivalent
950	0.699	332.025

Table 8
Future Prospective GHG emissions reduction (AMTP).

20 % of AMTP's energy demand (MWh)	Carbon intensity of electricity ($kgCO_2$/kwh)	Future Prospective GHG emissions reduction (tonnes CO_2 equivalent
609	0.299	182

the electrical cabinets of the Control system produce the highest impact on human health and ecosystem quality which is due to its composition consisting of steel, polyvinylchloride (PVC) plastic, printed wiring boards and cables. This is confirmed by a study which found that PVC which is commonly used in electrical cable construction for insulation, strength and protection has negative impacts on human health and the environment [40]. Life cycle assessment was conducted which showed that PVC manufacturing resulted in high global warming and acidification potential. The manufacturing process of PVC releases toxic chemical substances such as vinyl chloride, dioxins and phthalates into the environment through water, land and air emissions. These chemicals are detrimental to both human and animal health and can cause respiratory diseases, nervous system disorders and reduction in immunity to diseases [41]. The next highest impact is from the shell-side inserts of the TES which comprises of a large amount of aluminium. The mining and processing of metals such as aluminium and iron which is used to make steel can increase their levels in the aquatic system (groundwater, rivers, lakes) and the environment through industrial waste effluents and sewage discharge. Studies on toxicology have found that aluminium can pose a major threat for humans, animals and plants in causing many diseases and human health problems [42].

The electrical cabinets and the shell-side inserts consists of a large amount of steel and aluminium which contributed to their high negative impact on human health & ecosystem quality. MAND's platform structure has the third highest environmental and human health impact due to the substantial amount of steel and concrete used in its construction. This is followed by the therminol 59 weighing around 2,077.5 kg and consisting of chemicals such as ethyl benzene, benzene and styrene which contributes to its human health, ecosystem quality and resources impact. The rotating platform and TES storage tank are made from significant amount of steel, while the mirrors and the receivers comprise of a large amount of glass and aluminium, respectively. Overall, the category with the highest impact was human health, followed by resources and then ecosystem quality for MAND's ASTEP system. This could be due to the carbon emissions produced during the manufacturing of aluminium and steel, leading to air pollution and resulting in respiratory and other human health impacts [43,44]. The pressure transducers and temperature sensors produced the lowest environmental impact due to the least amount of materials and energy used in their manufacturing process.

Fig. 8 depicts the human health, ecosystem quality & resources impact of the components of AMTP's ASTEP system. The shell-side inserts of the TES produced the highest impact, followed by the electrical cabinet, TES storage tanks, mirrors, phase change materials and the receivers. The shell-side inserts had the greatest impact due to the large amount of aluminium and energy used in its manufacturing. There was 2,928 kg of aluminium used in AMTP's two TES tanks compared to 1.464 kg of aluminium used in a single TES tank for MAND. The manufacturing of aluminium is very energy intensive, which is mainly due to the extraction of alumina from bauxite and turning it into aluminium through smelters and electric induction furnaces using energy from fossil fuels which causes air pollution and is detrimental to human health and the environment [44]. The second highest impact is from the electrical cabinet due to the large amount of steel as well as PVC plastic used in its construction which are detrimental to human health and ecosystem quality. The third largest impact is from the TES storage tanks due to AMTP using two TES tanks, resulting in greater impact on ecosystem quality, resources and human health from the large amount of steel used in its manufacturing. The heat transfer fluid (therminol 59) has the fourth highest human health, resources and ecosystem quality impact due to the chemicals used in its production which can be harmful to human health and ecosystem quality [45]. The receivers and rotating platform also produce substantial impact on human health and resources as a result of the amount of steel and energy used in their production. The temperature sensors, valves and pressure transducers produce the lowest impact due to the less quantity of materials and energy used in their manufacturing.

Overall, it can be seen that AMTP's ASTEP system produces higher

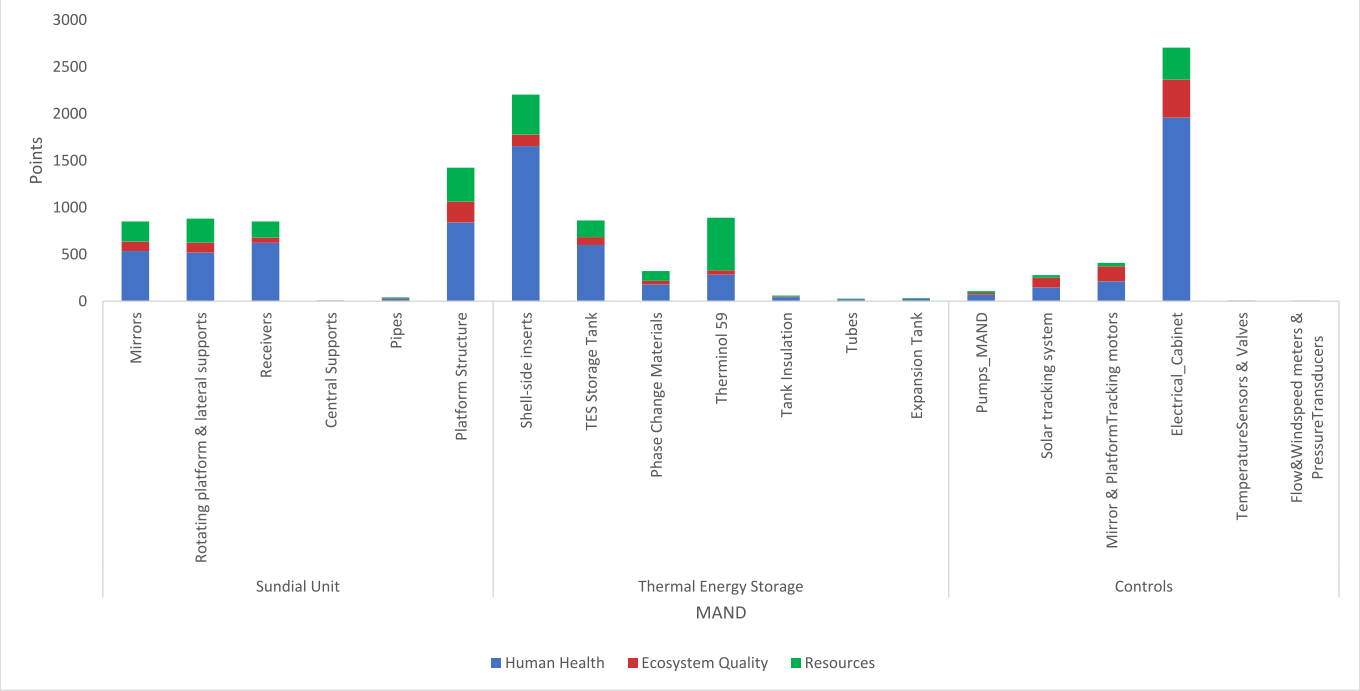

Fig. 7. Human health, ecosystem quality & resources impact of components of ASTEP system (MAND).

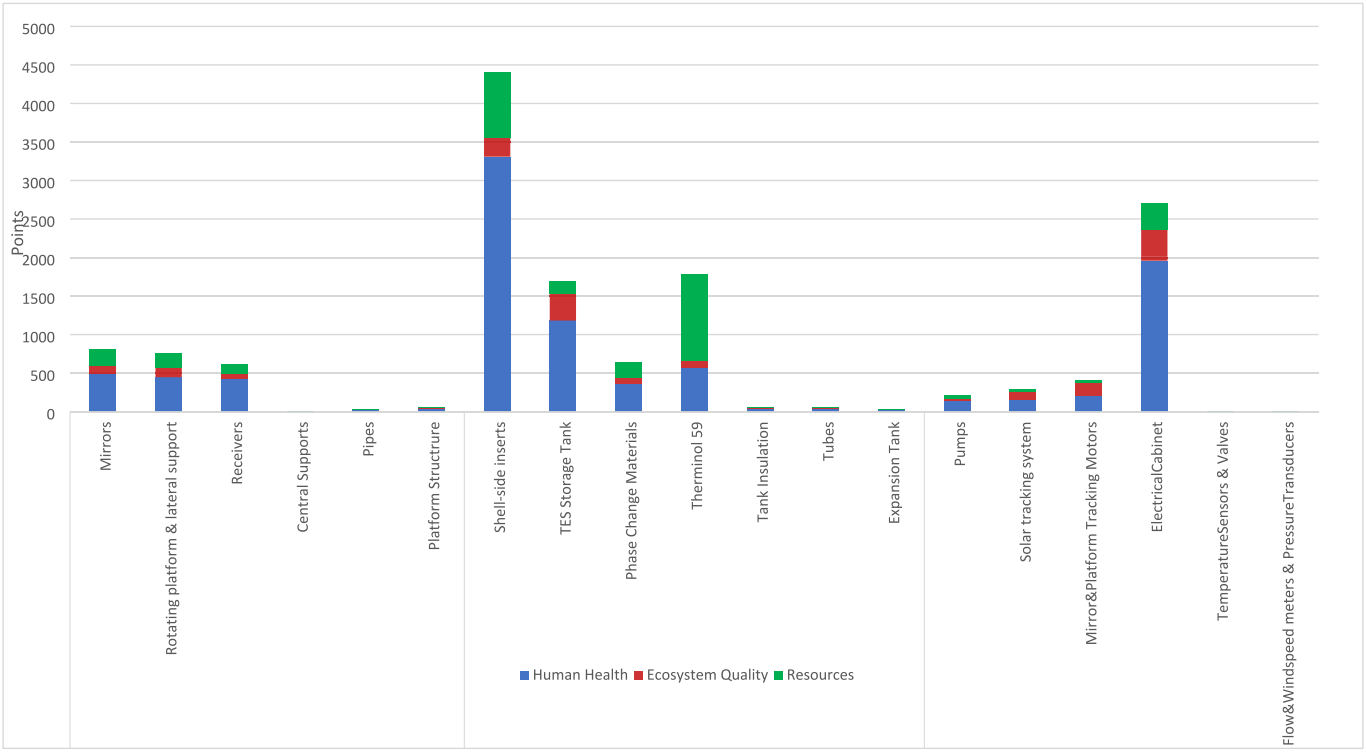

Fig. 8. Human health, ecosystem quality & resources impact of components of ASTEP system (AMTP).

impact on human health, resources and ecosystem quality than MAND's ASTEP system. This is mainly due to AMTP using two TES tanks compared to MAND's single TES tank, resulting in double the amount of aluminium shell-side inserts and energy used in their manufacturing process. Overall, the TES components generated the highest human health, ecosystem quality and resources impact, followed by the Controls and then the Sundial unit for both MAND and AMTP. This can be attributed to aluminium and steel being the largest amount of materials used in the manufacturing of the TES components and the electrical cabinet of the ASTEP system. For the Sundial unit, more mirrors were used for MAND's ASTEP system than for AMTP, resulting in the human health, ecosystem quality and resources impact of MAND's mirrors being slightly higher than AMTP. In addition, a significant amount of steel and concrete were used for the platform structure for MAND's ASTEP system compared to AMTP. This led to the construction of MAND's platform producing greater human health, ecosystem quality and resources impact than AMTP's platform.

4.2. *Cumulative energy demand of ASTEP system*

The cumulative energy demand (CED) of the ASTEP system is depicted in Fig. 9with the red colour representing the CED of MAND's ASTEP system and the blue colour representing the CED of AMTP's ASTEP system. The calculation consists of the total CED of the manufacturing, transportation, operation and waste disposal of the Sundial, TES, Controls as well as the platform structures of the ASTEP system. It can be seen that the TES has the highest CED, followed by the Sundial, the Controls and then the platform structures. AMTP's TES had

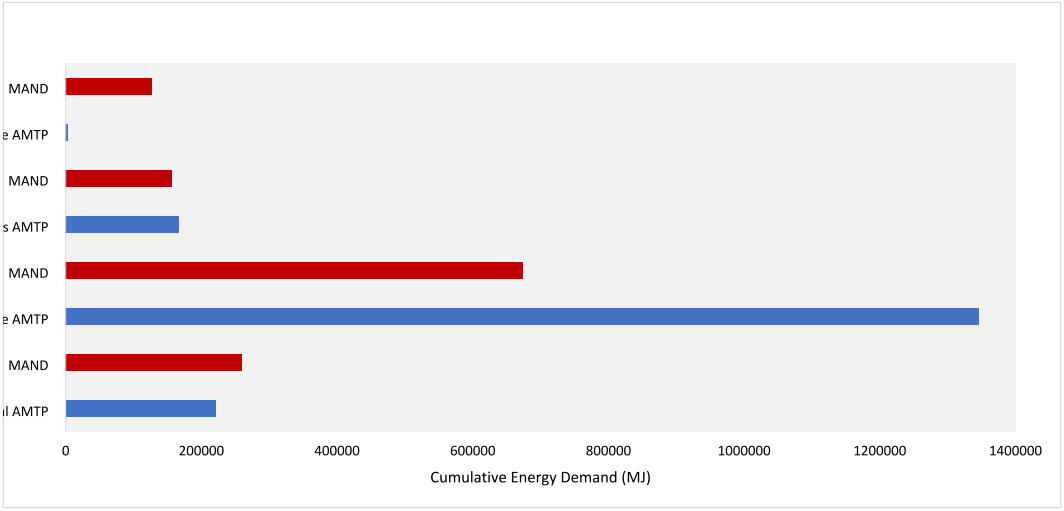

Fig. 9. Cumulative Energy Demand of ASTEP system (MAND & AMTP).

greater CED than MAND because AMTP uses two TES tanks compared to one TES tank used for MAND as it is more challenging for AMTP's ASTEP system to achieve a high temperature at its location of high latitude. Therefore, two TES tanks were required to enable AMTP's ASTEP system to provide temperatures up to 230 °C during days of high solar irradiation but achieve more constant temperatures on regular days. Consequently, the two TES tanks at AMTP results in double energy demand which is mainly due to the production of the aluminium shell-side inserts, phase change materials and the steel storage tanks. There was a total of 2,928 kg of aluminium used in the manufacturing of shell-side inserts for the two TES storage tanks, whilst half of that amount was used for MAND's single TES tank. This contributed to the significant cumulative energy demand of AMTP's TES tanks shown in Fig. 9 as aluminium is the most energy-intensive base metal to produce, with 1 tonne of aluminium requiring about 15 MWh of electricity [46]. Electricity consumption to run smelters constitutes the major part of energy consumption in aluminium primary production and grid electricity often uses fossil fuels as its energy source since around 50 % of aluminium used around the world including Europe, is made in China [44].

MAND' Sundial had higher CED than AMTP due to its design which required more components and materials than AMTP. A single-axis solar tracking system was used for MAND's Sundial as its location has high solar irradiance throughout the year. In contrast, a double-axis tracking system was used for AMTP's Sundial due to its high latitude location and lower solar irradiance. MAND's Sundial has 8 mirror lines compared to 6 mirror lines for AMTP's Sundial. In addition, a larger number of platform tubes were used for MAND's Sundial due to its design which required its mirrors and receivers to be located at different longitudinal positions. MAND's Sundial also had double the amount of lateral supports than AMTP; 20 lateral supports used for MAND compared to 10 lateral supports for AMTP's Sundial [47]. This contributed to MAND's Sundial requiring more materials and having a heavier concentrator than AMTP's Sundial, resulting in higher energy consumption in the manufacturing of its components. The double-axis solar tracking system used for AMTP's Sundial resulted in its Sundial design being simpler, lighter and using less materials than MAND's Sundial which used 20 % more materials than AMTP leading to greater CED in the manufacturing and transportation of its components. AMTP's Controls had higher CED than MAND's Controls as it used a double-axis solar tracking system compared to a single-axis solar tracking system for MAND. Overall, the Controls of the ASTEP system achieved lower CED than the TES and Sundial, due to less amount of materials and components used in the manufacturing of the Controls. MAND's platform structure for the ASTEP system had higher CED than AMTP as it used large amount of steel and concrete in its manufacturing process compared to AMTP's platform structure which only used concrete and no steel. 60 % of steel is made through the conventional blast furnace-basic oxygen furnace production method which is highly energy-intensive and consumes around 20–30 GJ of energy per 1 tonne of steel, resulting in the high CED and GHG emissions of steel production [48].

4.3. Greenhouse gas emissions (GHG) of the life cycle phases of the ASTEP system

The greenhouse gas emissions of each of the life cycle phases of the ASTEP system for MAND and AMTP are displayed in Fig. 10 and discussed in this section.

Fig. 10 shows the GHG emissions of the life cycle phases of ASTEP system for both MAND and AMTP. The manufacturing phase of the ASTEP system produced the highest GHG emissions followed by the operation, transportation and then the waste disposal phase of the components at their end of life stage. This is corroborated by studies in the literature which showed that the manufacturing of solar thermal systems generated the highest GHG emissions, followed by the operation and maintenance, whilst the disposal phase produced the lowest GHG emissions [49–51]. The manufacturing of the TES produced the greatest GHG emissions for both end-users, followed by the Sundial and the Controls. The manufacturing of AMTP's TES system produced greater GHG emissions than MAND, due to two TES tanks being manufactured for AMTP compared to a single TES tank manufactured for MAND's ASTEP system. The largest amount of material used in the manufacture of the TES system is aluminium, which was used mainly for the shell-side inserts. Aluminium production is carbon-intensive emitting 6.7 kg of carbon-dioxide emissions per kg of aluminium which contributed to the high GHG emissions of the manufacturing of the TES system [43]. A large amount of steel was also used in the manufacturing of the TES

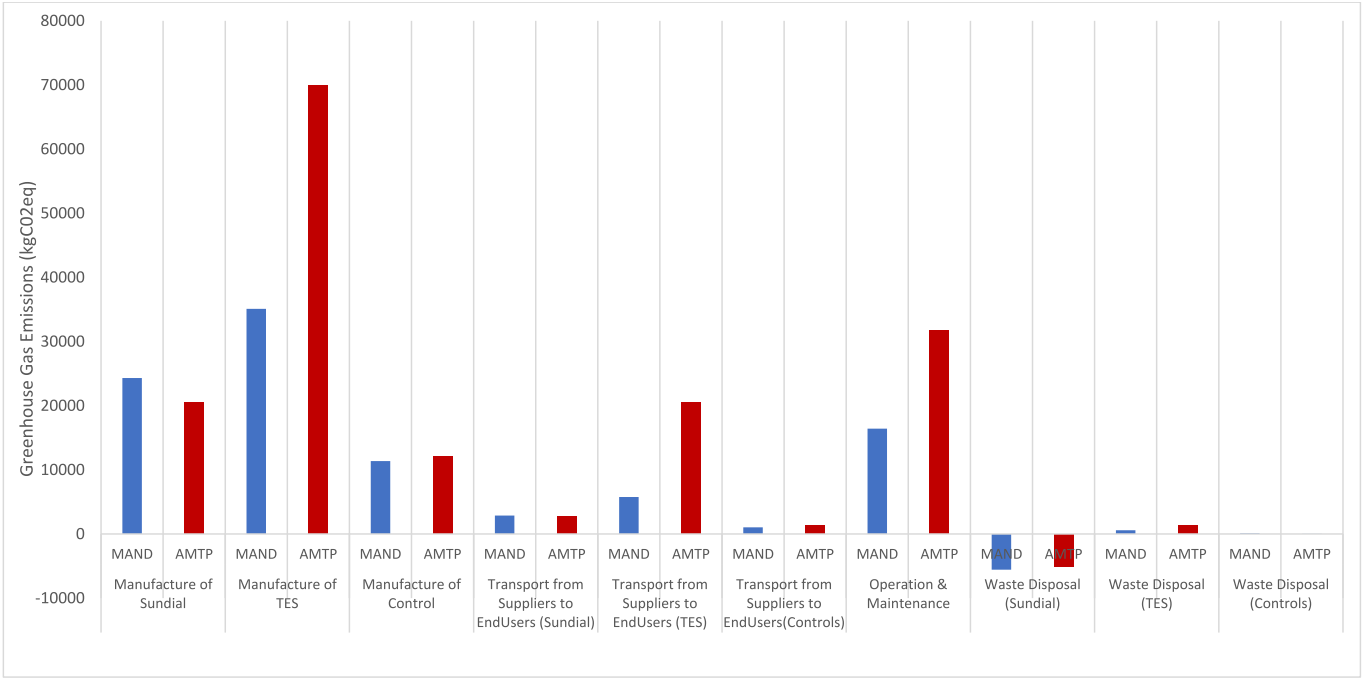

Fig. 10. GHG emissions of life cycle phases of ASTEP system.

tanks. The manufacturing of MAND's Sundial generated higher GHG emissions than AMTP as 20 % more materials were used in the manufacturing of its Sundial. A large quantity of steel was used in the manufacture of the Sundial unit, mainly for the rotating platform and the mirrors' supporting structures. Steel and concrete were used for MAND's ASTEP platform structure, with steel constituting the largest amount of materials used. In contrast, AMTP's ASTEP platform structure used only concrete. Conventional blast furnace-basic oxygen furnace is usually used in the production of crude steel, emitting around 1.6–2 tonnes of CO_2 per tonne of crude steel produced and contributing to the high GHG emissions of the raw materials processing of steel [43]. The GHG emissions produced by the manufacturing of the controls for both end users is minimal due to the lower quantity of the materials and energy used in the production of the Controls compared to the Sundial and the TES system.

It can be seen for the transportation phase, that transporting the TES components from suppliers to end-users generated the highest emissions, followed by the Sundial and then the Controls. Overall, the transportation of AMTP's ASTEP system produced higher emissions than MAND, due to AMTP having two TES tanks, making its ASTEP system heavier as well as AMTP being located a further distance from the suppliers and the place of assembly than MAND. For the operation phase, MAND's ASTEP system produced higher GHG emissions than AMTP, due to MAND's location of low latitude and higher solar irradiance resulting in it receiving more hours of solar irradiance than AMTP. This led to MAND's ASTEP system annual operating hours being higher than AMTP, resulting in its pumps and electric motors operating for longer periods, thereby consuming more electricity than AMTP's ASTEP system. The waste disposal of the ASTEP system for both end-users generated the least GHG emissions due to the recycling of the components at their end of life stage. This has been corroborated in the literature which found that the waste disposal phase at the end of life stage, generates the lowest environmental impact of a CSP plant, whilst the manufacturing phase produces the highest environmental impact [11,49,51].

Aluminium and steel were the main materials used in the manufacturing of the ASTEP system particularly for the TES and the Sundial. Aluminium is a durable metal which can be recycled infinitely without losing its quality and properties. Increasing the recycling rates of metals such as aluminium and steel contributes to reducing energy consumption and greenhouse gas emissions and is essential in the decarbonization of the aluminium and steel industry [43]. This is because 90 % of energy is saved during production when recycled aluminium is used compared to virgin aluminium material [52]. Steel can also be reused or recycled which is better for the environment and produces 80 % less carbon emissions than the production of primary crude steel [53]. The EU has set a target to become climate neutral by 2050 and consequently has implemented the new circular economy action plan which encourages sustainable consumption, promotes circular economy processes and aims to prevent waste through the reuse and recycling of materials [54]. This new circular economy action plan aims to achieve a carbon–neutral, environmentally sustainable, toxic-free and fully circular economy by 2050 with more stringent recycling rules in the EU [55]. The ASTEP system is currently being built and is expected to be completed and installed at MAND and AMTP in 2024. However, due to unforeseen delays in the construction and testing of the system, the ASTEP system was not completed in 2024 as planned. Construction of the system has now been completed in 2025 and the ASTEP system will be transported and installed at MAND and AMTP this year. The expected lifetime of the ASTEP system is 30 years which means the end of life waste disposal of its components are likely to occur in 2054 by which time EU countries should have achieved climate neutrality with the objectives of the circular economy action plan fully implemented. Therefore, all waste materials will be expected to be reused or recycled in line with the EU's circular economy plan.

4.4. Comparing the environmental impact of end-users' processes when ASTEP system and fossil-fuel used as energy sources

Fig. 11 compares the GHG emissions produced when fossil-fuels, Sundial (current capacity) and Sundial (at 15 % capacity of end users' energy demand) are used to supply thermal energy to MAND and AMTP's processes. The fossil-fuel used for AMTP's processes is electricity; 3,046.4 MWh of electricity is supplied annually to the oven to heat up the metal pipes in the factory. For MAND, electricity and LPG are used for their processes, resulting in total energy consumption of 4,749.5 MWh annually. The Sundial provides a fraction of this amount, at 27.8 MWh of annual thermal energy for MAND and AMTP's processes. The capacity of the Sundial is then increased to meet 15 % of AMTP and MAND's processes and the results are shown in Fig. 11. It can be seen that the GHG emissions of AMTP and MAND's processes is highest when fossil fuel energy sources are used. This amount reduces when the Sundial (current capacity) is used to provide thermal energy for AMTP and MAND's processes. A larger reduction in the GHG emissions is observed when the capacity of the Sundial is increased to meet 15 % of AMTP and MAND's energy demand.

5. Future prospective of GHG emissions reduction of the ASTEP system

Table 9 shows the current and future prospective capacity of the ASTEP system for MAND and AMTP along with their GHG emissions reduction. It can be seen that when the current capacity of the ASTEP system for MAND is increased from 27.8 MWh to a future capacity of 950 MWh, its CO_2 emissions reduction rises from 9.7 tonnes to 332 tonnes of CO_2 emissions. Likewise, when the current capacity of the ASTEP system for AMTP is increased from 27.8 MWh to a future capacity of 609 MWh, its CO_2 emissions reduction rises from 8.3 tonnes to 182 tonnes of CO_2 emissions. This demonstrates the potential of the GHG emissions reduction of the ASTEP system when it is used to provide thermal energy to industrial processes at large capacities. However, in order to provide thermal energy at capacities of up to 950MWh, the ASTEP system may experience a substantial increase in the number and size of its components leading to higher land space requirements. Concentrating solar power (CSP) plants require large areas of land for the deployment of the solar field, thermal storage and power block [56]. Tahir et al. [57] reported the typical land area requirements for different CSP technologies which showed that LFR had the lowest land use requirement at 2 acres/MW, followed by parabolic dish at 2.8 acres/MW, parabolic trough at 6.2 acres/MW and then solar tower at 8.9 acres/MW. This suggests that linear Fresnel technologies require the least land space compared to the other solar thermal technologies [57]. Furthermore, the use of LFR technology to provide thermal energy to industrial processes has several advantages compared to other solar thermal technologies. This include its simplicity, robustness, low wind load, lower land use requirements and lower capital costs [58].

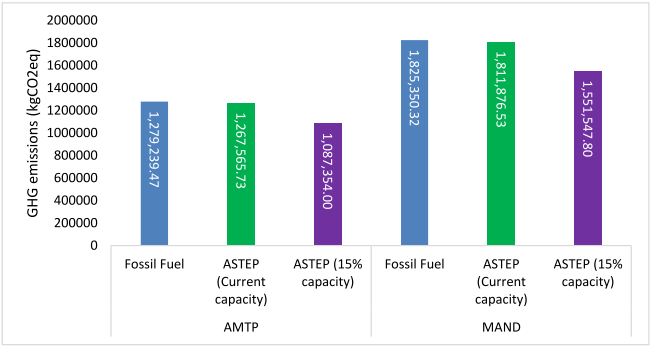

Fig. 11. GHG emissions of AMTP & MAND's processes when different energy sources are used.

Table 9
Future Prospective Capacity & GHG Emissions Reduction of the ASTEP system.

ASTEP System	MAND		AMTP	
	Current Capacity	Future Prospective Capacity	Current Capacity	Future Prospective Capacity
Energy provided (MWh/year)	27.8	950	27.8	609
GHG Emissions Reduction	9.7 tonnes of CO_2 equivalent	332 tonnes of CO_2 equivalent	8.3 tonnes of CO_2 equivalent	182 tonnes of CO_2 equivalent

6. Conclusion

The assessment of the environmental impact of an innovative ASTEP solar thermal system and its application to two different industrial processes showed multiple benefits from environmental, technical and economic aspects. Its technical benefits include ability to provide thermal energy up to 400 °C for industrial processes at locations of low and high latitudes where other solar thermal systems may be limited to operate. The environmental benefits of the ASTEP system is its ability to contribute to the decarbonisation of industries, particularly when in applied in a larger capacity. ASTEP system could provide 27.8 MWh of thermal energy to both MAND and AMTP's processes, respectively reducing their GHG emissions by 9.7 tonnes and 8.3 tonnes of CO_2 equivalent. By expanding the capacity of the ASTEP system to 950 MWh for MAND and 609 MWh for AMTP, providing 20 % of their energy demand, the annual reduction of CO_2 emissions is 328 and 182 tonnes CO_2 equivalent for MAND and AMTP, respectively. This demonstrates the great potential of the ASTEP system to reduce CO_2 emissions of industrial processes, which could play an important role in the decarbonization of EU industries. Future research can be conducted on the environmental LCA impact of water consumed during the operational phase of the ASTEP system to achieve a comprehensive evaluation of its environmental performance covering both energy and water consumption of the system. Future work should also focus on the environmental impact of LFRs of different plant capacity used to supply thermal energy in industrial processes to enable comparisons to be made with other technologies, as well as the ASTEP solar thermal system.

CRediT authorship contribution statement

Lisa Baindu Gobio-Thomas: Supervision. **Mohamed Darwish:** Supervision. **Antonio Rovira:** Supervision. **Ruben Abbas:** Supervision. **Juan Pedro Solano:** Supervision. **Jose Munoz Camara:** Supervision. **Peter Kew:** Supervision. **Krzysztof Naplocha:** Supervision. **Valentina Stojceska:** Supervision.

Declaration of competing interest

The authors declare that they have no known competing financial interests or personal relationships that could have appeared to influence the work reported in this paper.

Acknowledgments

This project is funded from the EU Horizon 2020 research and innovation programme, Application of Solar Energy in Industrial processes (ASTEP), under grant agreement No 884411.

References

[1] M.H. Ahmadi, M. Ghazvini, M. Sadeghzadeh, M.A. Nazari, R. Kumar, A. Naeimi, T. Ming, Solar power technology for electricity generation: a critical review, Energy Sci. Eng. 6 (2018) 340–361, https://doi.org/10.1002/ese3.239.
[2] UNFCCC, 2022. About the Secretariat. Available at: About the Secretariat | UNFCCC. [Accessed on 17th May 2022].
[3] European Commission, 2022. EU Climate targets: how to decarbonise the steel industry. Available at: EU climate targets: how to decarbonise the steel industry (europa.eu). [Accessed on 6th February 2022].
[4] European Commission, 2022a. 2030 Climate Target Plan. Available at: https://ec.europa.eu/clima/eu-action/european-green-deal/2030-climate-target-plan_en. [Accessed on 25th January 2022].
[5] EuroStat, 2023. Energy Statistics- an overview. Available at: https://ec.europa.eu/eurostat/statistics-explained/index.php?title=Energy_statistics_-_an_overview#Final_energy_consumption. [Accessed on 10th June 2023].
[6] J. Brodny, M. Tutak, Analysis of the efficiency and structure of energy consumption in the industrial sector in the European Union countries between 1995 and 2019, Sci. Total Environ. 808 (2022) 152052, https://doi.org/10.1016/j.scitotenv.2021.152052.
[7] European Commission, 2021. Heating & Cooling. Available at: https://ec.europa.eu/energy/topics/energy-efficiency/heating-and-cooling_en. [Accessed on 28th July 2021].
[8] IEA, 2020. European Union 2020: Energy Policy Review. Available at: https://www.iea.org/reports/european-union-2020 [Accessed on 28th November 2021].
[9] European Parliament, 2020. Energy-intensive industries. Available: *Energy-intensive industries (europa.eu). [Accessed on 29th May 2023].
[10] H. Tannous, V. Stojceska, A.S. Tassou, The use of solar thermal heating in SPIRE and Non-SPIRE industrial processes, Sustainability 15 (10) (2023) 7807, https://doi.org/10.3390/su15107807.
[11] S.J.W. Klein, E.S. Rubin, Life cycle assessment of greenhouse gas emissions, water and land use for concentrated solar power plants with different energy backup systems, Energy Policy 63 (2013) 935–950, https://doi.org/10.1016/j.enpol.2013.08.057.
[12] T. Telsnig, G. Weinrebe, J. Finkbeiner, L. Eltrop, Life cycle assessment of a future central receiver solar power plant and autonomous operated heliostat concepts, Sol. Energy 157 (2017) 187–200, https://doi.org/10.1016/j.solener.2017.08.018.
[13] L. Salisu, J.S. Enaburekhan, A.A. Adamu, Techno-economic and life cycle analysis of energy generation using concentrated solar power (CSP) technology in sokoto state, Nigeria, J. Appl. Sci. Environ. Manage. 23 (5) (2019) 775, https://doi.org/10.4314/jasem.v23i5.1.
[14] K. Hirbodi, M. Enjavi-Arsanjani, M. Yaghoubi, Techno-economic assessment and environmental impact of concentrating solar power plants in Iran, Renew. Sustain. Energy Rev. 120 (2020) 109642, https://doi.org/10.1016/j.rser.2019.109642.
[15] S. Banacloche, I. Herrera, Y. Lechón, Towards energy transition in Tunisia: sustainability assessment of a hybrid concentrated solar power and biomass plant, Sci. Total Environ. 744 (2020), https://doi.org/10.1016/j.scitotenv.2020.140729.
[16] G.N. Kulkarni, S.B. Kedare, S. Bandyopadhyay, Design of solar thermal systems utilizing pressurized hot water storage for industrial applications, Sol. Energy 82 (8) (2008) 686–699, https://doi.org/10.1016/j.solener.2008.02.011.
[17] V. Piemonte, M. de Falco, A. Giaconia, P. Tarquini, G. Iaquaniello, Life cycle assessment of a concentrated solar power plant for the production of enriched methane by steam reforming process, Chem. Eng. Trans. 21 (2010) 25–30, https://doi.org/10.3303/CET1021005.
[18] Hang, Y., Balkoski,K. and Meduri, P. (2013). Life Cycle Analysis of Linear Fresnel Solar Power Technology. In ASME Power Conference, Boston, Massachusetts, USA, 29 July – 1 August 2013.
[19] Kizilkan, O., Kabul, A. and Dincer, I. (2016). Development and performance assessment of a parabolic trough solar collector-based integrated system for an ice-cream factory. Doi: 10.1016/j.energy.2016.01.098.
[20] Kuenlin, A., Augsburger, G., Gerber, L. and Maréchal, F. (2013). Life cycle assessment and environomic optimization of concentrating solar thermal power plants. *Proceedings of the 26th International Conference on Efficiency, Cost, Optimization, Simulation and Environmental Impact of Energy Systems*, ECOS2013, Guilin, China, 16-19 July.
[21] Y.N. Dabwan, G. Pei, G. Gao, J. Li, J. Feng, Performance analysis of integrated linear fresnel reflector with a conventional cooling, heat, and power tri-generation plant, Renew. Energy 138 (2019) 639–650, https://doi.org/10.1016/j.renene.2019.01.098.
[22] S. Mihoub, Design, economic, and environmental assessments of linear Fresnel solar power plants, Environ. Prog. Sustain. Energy 39 (3) (2019) 13350, https://doi.org/10.1002/ep.13350.
[23] M. Ghodbane, E. Bellos, Z. Said, B. Boumeddane, A. Khechekhouche, M. Sheikholeslami, Z.M. Ali, Energy, Financial, and Environmental Investigation of a Direct Steam Production Power Plant Driven by Linear Fresnel Solar Reflectors, J. Sol. Eng. 143 (2020), https://doi.org/10.1115/1.4048158.
[24] E. Batuecas, S. Taramona, J. Gomez-Hernandez, J.V. Briongos, Environmental and energetic behavior of a Beam-down linear Fresnel solar field for low-grade thermal energy applications, Appl. Therm. Eng. 231 (2023) 121002, https://doi.org/10.1016/j.applthermaleng.2023.121002.
[25] L.B. Gobio-Thomas, M. Darwish, V. Stojceska, Environmental impacts on solar thermal power plants used in industrial supply chains, Therm. Sci. Eng. Prog. 38 (2023) 101670, https://doi.org/10.1016/j.tsep.2023.101670.

[26] R. Abbas, R. Barbera, A. Rovira, M. Barnetche, Sundial, a new collector for solar heat for industrial processes: Optical and thermal design, Therm. Sci. Eng. Prog. 44 (2023) 102025, https://doi.org/10.1016/j.tsep.2023.102025.
[27] ASTEP, 2019. Application of Solar Thermal Energy to Processes (ASTEP). Horizon 2020.
[28] Ibarra, M., Barnetche, M., Barbero, R., Gonzalez-Portillo, L.F., Abbas, R. and Rovira, A. (2021). Design and integration of a solar heat system based on the Sundial for industrial processes. *SolarPACES Conference.* Online, 27th September – 1st October 2021.
[29] Fernández, J.P.S., Camara, J.M. and Hammou, H. (2021). D4.1 Engineering configuration of the thermal energy storage system. Available at: https://astepproject.eu/wp-content/uploads/2022/01/ASTEP_D4.1_Engineering-configuration-of-the-thermal-energy-storage-system_V1.0_211115_UPCT.pdf. [Accessed on 18th September 2023].
[30] J. Oller, I. Kakogiannos, J. Vincente, A. Torres, D3.5 Control strategy for Sundial systems, D4.5 Control strategy for hybrid TES system, D5.3 Integrated Control strategies & framework for ASTEP combined systems, ASTEP (2021).
[31] British Standards Institution, BS 14001:2015 Environmental management systems – Requirements with guidance for use, British Standards Institution, London, 2015.
[32] Abbas, R., Rovira, A., Ibarra, M., Barnetche, M., Barbero, R., Portillo, L.F.G., Palacios, E., Marcos, J.D. (2021). D3.3 Design of the daily and yearly operation for AMTP and MAND. D5.1 Report on the integrated ASTEP model development and Conceptual Designs. Application of Solar Thermal Energy to Processes. Available at: https://astepproject.eu/wp-content/uploads/2022/02/ASTEP_D3.3-Report_on_the_integrated_ASTEP_model_development_and_Conceptual_Designs_V2.1_220119_UPM.pdf. [Accessed on 19th September 2023].
[33] C. Marugán-Cruz, D. Serrano, J. Gómez-Hernández, S. Sánchez-Delgado, Solar multiple optimization of a DSG linear Fresnel power plant, Energ. Conver. Manage. 184 (2019) 571–580, https://doi.org/10.1016/j.enconman.2019.01.054.
[34] G. Gasa, A. Lopez-Roman, C. Prieto, L.F. Cabeza, Life cycle assessment (LCA) of a concentrating solar power (CSP) plant in tower configuration with and without thermal energy storage (TES), Sustainability 13 (2021), https://doi.org/10.3390/su13073672.
[35] Engineering Toolbox, 2022. Combustion of Fuels – Carbon Dioxide Emission. Available at: https://www.engineeringtoolbox.com/co2-emission-fuels-d_1085.html. [Accessed on 24th November 2022].
[36] Nardini, S., Buonomo, B., Manca, O., Tannous, H., Masera, K., Tassou, S and Stojceska, V. (2020). D2.2 Level 2 End-user and context analysis report (ASTEP).
[37] Momi, S.A., Dutta, M., Hassan, S., Karder, G. and Iftakher, S. (2016). Study of LPG (Liquefied Petroleum Gas) and CNG (Compressed Natural Gas) Vehicles and its Future Aspects. *International Conference on Mechanical, Industrial & Energy Engineering.* Khulna, Bangladesh, 26-27 December.
[38] EonNext, 2022. How to convert gas units to kwh. Available at: https://www.eonnext.com/business/help/convert-gas-units-to-kwh. [Accessed on 29th October 2022].
[39] UnitConverters, 2022. Convert Megajoule to Kilowatt-hour. Available: https://www.unitconverters.net/energy/megajoule-to-kilowatt-hour.htm. [Accessed on 29th October 2022].
[40] Comanita, E.D., Ghinea, C., Rosca, M., Simion, I.M., Petratru, M., Gavrilescu, M. (2015). Environmental Impacts of Polyvinyl Chloride (PVC) Production Process. *The 5th IEEE International Conference on E-Health and Bioengineering*, Grigore T. Popa University of Medicine and Pharmacy, Iasi, Romania, 19th -21st November.
[41] R. Proshad, T. Kormoker, S. Islam, M.A. Haque, M. Rahman, M.R. Mithu, Toxic effects of plastic on human health and environment: a consequences of health risk assessment in Bangladesh, Int. J. Health 6 (1) (2018) 1–5. https://doi.org/10.14419/ijh.v6i1.8655.
[42] A.I. Pogue, W.J. Lukiw, Aluminium, the genetic apparatus of the human CNS & Alzheimer's disease (AD), Morphologie 100 (2016) 56–64, https://doi.org/10.1016/j.morpho.2016.01.001.
[43] European Aluminium, 2019. Vision 2050: European Aluminum Contribution to the EU's Mid-Century Low-Carbon Roadmap. Available at: sample_vision-2050-low-carbon-strategy_20190401.pdf (european-aluminium.eu). [Accessed on 19th June 2023].
[44] World Economic Forum, 2023. Aluminium Industry. Available: Aluminium Industry - The Net-Zero Industry Tracker | World Economic Forum (weforum.org).
[45] M. Bosnjakovic, V. Tadijanovic, Environment Impact of a Concentrated Solar Power Plant, Tech. J. 13 (2019) 68–74.
[46] ING, 2023. Aluminium smelter shutdowns threaten Europe's green transition. Available at: Aluminium smelter shutdowns threaten Europe's green transition | Article | ING Think. [Accessed on 2nd June 2023].
[47] R. Abbas, M. Valdes, A. Sebastian, D3.6 report on the detailed design of Sundial for both end users. Application of Solar Thermal Energy to Processes (ASTEP), 2022.
[48] M. Shahabuddin, G. Brooks, M. Rhamdhani, A., Decarbonisation and hydrogen integration of steel industries: recent development, challenges and technoeconomic analysis, J. Clean. Prod. 395 (2023) 136391, https://doi.org/10.1016/j.jclepro.2023.136391.
[49] J.J. Burkhardt, G.A. Heath, C.S. Turchi, Life cycle assessment of a parabolic trough concentrating solar power plant and the impacts of key design alternatives, Environ. Sci. Tech. 45 (2011) 2457–2464, https://doi.org/10.1021/es1033266.
[50] G. San Miguel, B. Corona, Hybridizing Concentrated Solar Power (CSP) with Biogas and Biomethane as an Alternative to Natural Gas: Analysis of Environmental Performance Using LCA, Renew. Energy. 66 (2014) 580–587, https://doi.org/10.1016/j.renene.2013.12.023.
[51] L. Abou El Kourom, L. Bahi, A. Bahi, Environmental impact analysis of concentrated solar power plants in Morroco, Int. J. Adv. Res. Eng. Technol. 11 (5) (2020) 461–468. 10.34218/IJARET.11.5.2020.047.
[52] Reinch, W.A and Benson, E. (2022). Decarbonizing Aluminium: Rolling out a more sustainable sector. Centre for Strategic & International Studies (CSIS).
[53] European Commission, 2020. Decarbonisation of industrial heat: The iron and steel sector. Joint Research Centre, European Union. Available at: https://setis.ec.europa.eu/decarbonisation-industrial-heat-iron-and-steel-sector_en. [Accessed on 24th June 2023].
[54] European Commission, 2023. Circular economy action plan. Available: https://environment.ec.europa.eu/strategy/circular-economy-action-plan_en. [Accessed on 5th June 2023].
[55] EU Monitor, 2023. Circular economy: definition, importance and benefits. Available at: https://www.eumonitor.eu/9353000/1/j9vvik7m1c3gyxp/vknegugz7hwu?ctx=vjxzjv7ta8z1. [Accessed on 11th June 2023].
[56] C. Sharma, A.K. Sharma, S.C. Mullick, T.C. Kandpal, Assessment of solar thermal power generation potential in India, Renew. Sustain. Energy Rev. 42 (2015) 902–912, https://doi.org/10.1016/j.rser.2014.10.059.
[57] S. Tahir, M. Ahmad, H.M. Abd-ur-Rehman, S. Shakir, Techno-economic assessment of concentrated solar thermal power generation and potential barriers in its deployment in pakistan, J. Clean. Prod. 293 (2021) 126125, https://doi.org/10.1016/J.JCLEPRO.2021.126125.
[58] J. Sun, Hybrid solar power system, in: A.K. Azad (Ed.), Advances in Clean Energy Technologies, Academic Press, 2021, pp. 405–448.